ACS SENSORS

pubs.acs.org/acssensors

Article

Wearable Analytical Platform with Enzyme-Modulated Dynamic Range for the Simultaneous Colorimetric Detection of Sweat Volume and Sweat Biomarkers

Andreu Vaquer, Enrique Barón,* and Roberto de la Rica*

Cite This: *ACS Sens.* 2021, 6, 130−136

Read Online

ACCESS | Metrics & More | Article Recommendations | Supporting Information

ABSTRACT: In this manuscript, we introduce a wearable analytical platform that simultaneously measures the concentration of sweat lactate and sample volume. It contains two sensors entirely made of filter paper that can be easily affixed on the skin with medical-grade tape. The lactate biosensor features a unique signal modulation mechanism that enables fine-tuning the dynamic range. It consists of adding a competitive enzyme inhibitor in different reservoirs. Thanks to this, it is possible to choose between a very low limit of detection (0.06 mM) and a linear response in the physiological concentration range (10−30 mM). The sweat volume sensor was obtained by adding a reservoir containing gold nanoparticles. As the wearer sweats, the nanoparticles are carried through a paper channel. This is used to gauge the volume of sample by measuring the distance traveled by the nanoprobes. Using fine-tuned lactate biosensors and combining them with the volume sensors allowed us to quantify variations in the levels of sweat lactate independently of the wearer's sweat rate during an exercise routine. The platform design can be customized to meet the end user's needs, which makes it ideal for developing a wide array of disposable wearable biosensors.

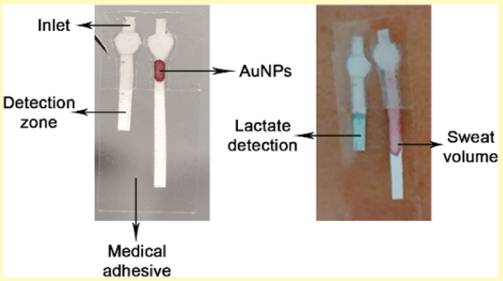

KEYWORDS: *paper-based analytical device, lactate, enzyme, wearable biosensor, nanoparticle, sweat*

Colorimetric biosensors are becoming increasingly popular because test results can be directly recorded with the camera of a mobile device.[1−3] This signal detection scheme is particularly useful for developing wearable biosensors for health self-monitoring that use the patient's smartphone as a reader.[4−9] In wearable sweat biosensors, a sensing patch is adhered to the patient skin.[10−15] As the patient sweats, perspiration provides a constant supply of analyte and carries reagents from reservoirs to detection areas without using pumps.[16−18] Fluids are typically transported through poly(dimethylsiloxane) (PDMS) channels or through wicking when the devices are made of paper.[19−22] These colorimetric wearable biosensors are inexpensive and easy to dispose of.[23,24] However, several challenges must be overcome before they can be used for health monitoring. First, the analytical performance of the device needs to be fine-tuned to quantify signals in the clinically relevant range. This can be challenging for highly sensitive biosensors whose signal may become saturated at physiological levels of analyte.[25,26] Furthermore, the intensity of the colorimetric signal depends not only on the concentration of analyte but also on the sample volume. When the sweat rate is unknown, it is not possible to elucidate the individual contribution of these factors to the measured colorimetric signals.[27−29] Consequently, signal quantification is not precise.[30]

In this manuscript, we introduce an analytical platform for fabricating colorimetric wearable biosensors that enables fine-tuning the dynamic range as well as correcting signal variations originating from varying sweat volumes. The detection platform consists of two adjacent sensors made entirely of paper whose inlets are in direct contact with the skin (Figure 1A,B). One sensor measures variations in the concentration of lactate as a model sweat biomarker, whereas the other one generates colorimetric signals that are directly related to the sweat volume. L-Lactate detection is accomplished through the peroxidase-mediated oxidation of 3,3′,5,5′-tetramethylbenzidine (TMB) using the H_2O_2 generated by lactate oxidase (LOX) as a cofactor (Figure 1C). The dynamic range of this lactate biosensor can be fine-tuned with a novel enzyme-modulated mechanism. It consists of adding a competitive inhibitor (D-lactate) in different reservoirs of the biosensor (R1 and R2, Figure 1C). This changes the apparent Michaelis constant (K_m) of LOX and makes enzyme activity dependent

Received: September 23, 2020
Accepted: December 14, 2020
Published: December 29, 2020

https://dx.doi.org/10.1021/acssensors.0c01980
ACS Sens. 2021, 6, 130−136

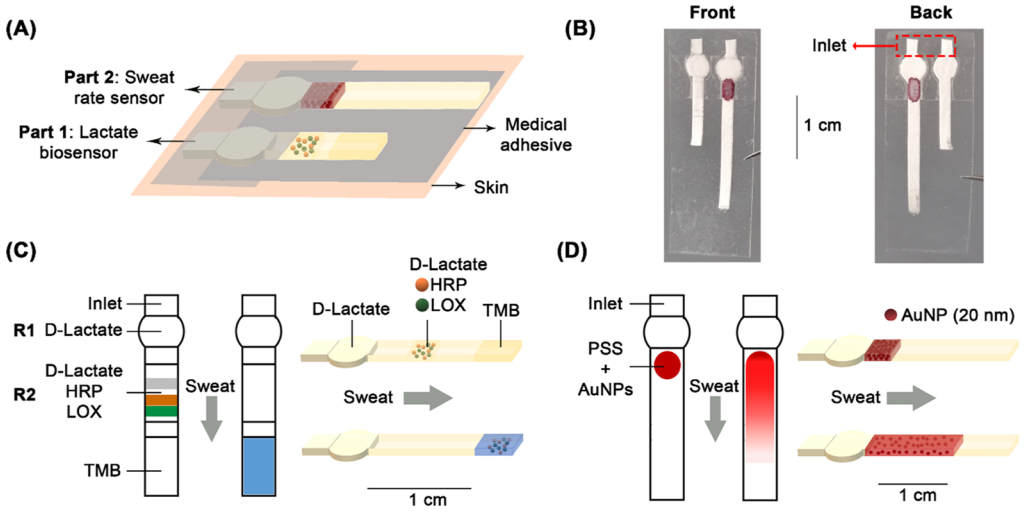

Figure 1. Design of the wearable analytical platform. (A) Schematic representation and (B) photographs of the platform. Medical adhesive below the paper strips prevents contact with the skin with the exception of the inlets. Another layer of medical adhesive above the strips presses the inlets against the skin. The area in contact with the skin is highlighted in red. (C) Lactate biosensor before and after sweat measurements. A circular area containing D-lactate is located right after the inlet (reservoir 1, R1). We chose this design to store large amounts of reagents in a short device. Another area containing D-lactate, horseradish peroxidase (HRP), and lactate oxidase (LOX) is located between the circular area and the detection zone (reservoir 2, R2). Finally, TMB is stored in the detection zone. (D) Sweat rate sensor before and after sweat measurements. A reservoir containing polystyrene sulfonate (PSS) and gold nanoparticles (AuNPs) is located right after the inlet.

on the concentration of L-lactate in the physiological range. The sweat volume sensor contains a reservoir for storing gold nanoparticles (Figure 1D). As the wearer sweats the nanoparticles are carried through the paper channel, which becomes stained by the plasmonic nanoprobes. This is used to gauge the volume of sample that has entered the wearable at a given time by measuring the length of the stained paper. Since the lactate biosensor and the sweat volume biosensor are placed in close vicinity, the distance traveled by the nanoparticles can be used to estimate the sample volume entering the lactate biosensor. This allows one to rectify the colorimetric signal from the lactate biosensor and make it less dependent on the volume of sample entering the device. Thanks to this we were able to measure lactate levels independently of the wearer's sweat rate during an exercise routine in a group of volunteers. Measurements obtained this way were in agreement with a reference method, which makes the proposed analytical platform promising for monitoring lactate levels in healthcare-related applications.

EXPERIMENTAL SECTION

Reagents. Sodium-L-lactate (≥99.0%), sodium-D-lactate (≥99.0%), 3,3′,5,5′-tetramethylbenzidine (TMB, ≥99%), poly(sodium 4-styrenesulfonate) (PSS, 30% in water), Tween 20, lactate oxidase (LOX) from *Aerococcus viridans* (500 U), horseradish peroxidase (HRP, Type VI-A, salt-free), and Whatman filter paper (Grade 41, 20 μm pore, cellulose, ashless) were purchased from Sigma-Aldrich (St. Louis, MO). Bovine serum albumin (BSA, protease-free) was purchased from VWR (Solon). Phosphate-buffered saline (PBS) containing 1 mg mL^{-1} BSA and 0.05% Tween 20 were prepared following standard procedures. Poly(ethylene glycol)-coated gold nanoparticles (PEG-AuNPs, 20 nm) were fabricated as described in the Supporting Information.

Fabrication of the Wearable Analytical Platform. *Wearable Device Part 1: Lactate Biosensor.* Whatman filter paper (pore size, 20 μm; Grade 41) was cut into 2 × 0.2 cm^2 strips and modified with a solution of BSA-Tween (1 mg mL^{-1} and 0.05% in PBS, respectively) to avoid nonspecific interactions between enzymes and the paper substrate. Modification was done by soaking the strips in the solution for 5 s and then drying them on an absorbent paper at room temperature. TMB (10 mM, 0.5 μL) was drop-cast at the end of the strip. A 0.5 μL drop of HRP (50 μg mL^{-1} in PBS) and LOX (600 μg mL^{-1} in PBS) was drop-cast 0.5 cm away from the TMB area (Figure 1C). Enzymes are carried by the sample flow and arrive at the detection area at the same time as the lactate analyte. The concentrations of TMB and LOX were optimized as shown in Figure S1. A 0.3 cm × 0.2 cm inlet in contact with the skin serves as the entry point for sweat. The rest of the device is covered with medical adhesive to isolate it from the skin (3M, Minnesota).

To fine-tune the biosensor dynamic range, D-lactate (1 M) was drop-cast in two different reservoirs of the paper biosensors. The first reservoir (R1) was placed in a circular area above the enzymes, while the second reservoir (R2) was the one containing the enzymes (Figure 1C). Different degrees of inhibition were accomplished by adding a different number of drops and letting them dry in the reservoirs. The three replicates refer to measurements performed with three independent sensors in all cases.

Wearable Device Part 2: Sweat Rate Sensor. Grade 41 filter paper (pore size 20 μm) from Whatman was cut into 3 × 0.2 cm^2 strips and modified with BSA and Tween to avoid nonspecific interactions as explained for part 1. Afterward, one drop (0.5 μL) of PSS (10%) was added and dried at room temperature.[31] Finally, 0.5 μL of AuNPs (1:2 dilution in PBS) was added into the same location. The concentrations of BSA-Tween, PSS, and AuNPs were optimized as shown in Figure S2. The sensor was calibrated by adding PBS of volumes between 3 and 9 μL and subsequently measuring the distance from the inlet to the flow end line using Adobe Photoshop. The sample enters the sensor through a 0.3 cm × 0.2 cm inlet (Figure 1D). The rest of the device is covered with medical adhesive to isolate it from the skin (3M, Minnesota). The three replicates refer to measurements performed with three independent sensors in all cases.

Assembly of the Analytical Platform. Both sensors were placed between two medical adhesives (3M, Minnesota) with a separation of 1 mm between them (Figures 1A and 4A). The bottom layer fixes the device to the skin, avoiding a direct contact of the device with the skin, with the exception of the inlets. The top layer covers the inlets and also presses them against the skin so that the sweat can enter the device by capillarity. The detection area is covered during storage to avoid the oxidation of TMB, but it is uncovered during the measurements because the enzymatic reaction needs O_2.

https://dx.doi.org/10.1021/acssensors.0c01980
ACS Sens. 2021, 6, 130−136

Colorimetric Signal Detection. Images were obtained with a Huawei P30 lite smartphone. A three-color reference pattern was used to compensate for changing light conditions. Figure S3 compares the colorimetric signals measured from images taken with a scanner (MFC-1910W, Brother) and with the smartphone camera. Pixel intensity (PI) profiles were obtained using ImageJ. In grayscale, the maximum pixel intensity (255) corresponds to pure white, while the minimum (0) corresponds to pure black. Colorimetric signal (S) was calculated by subtracting the PI from 255. This yields an inverted signal in comparison to the raw data.

Sweat Lactate Measurements. The device was applied to five healthy volunteers during a stationary bicycle routine. It consisted of a 15 min warm-up followed by gradual increases of the workload, to increase the heart rate. The aim was to achieve three conditions, as defined by the beats per minute (bpm): low (<110 bpm), moderate (~130 bpm), and intense (>150 bpm). Blood and sweat lactate levels change under aerobic (110−130 bpm) and anaerobic (>150 bpm) conditions.[32] The device was removed from the skin when the AuNPs red mark reached the desired volume (6−8 μL) to avoid the saturation of the enzymatic signal. The protocol was approved by the Balearic Islands Ethics Committee (IB 4053/19 PI). Informed consent was given by all participants.

In addition to the measurements with the wearable device, sweat drops were also manually collected using an Eppendorf tube and the lactate concentration was determined with the method explained in Figure S4. This method was validated in artificial sweat samples and showed good linearity (r^2 = 0.996), accuracy (98−102%), and reproducibility (relative standard deviation (RSD) 2−8%) in the concentration range between 0 and 1 mM. Therefore, it was considered suitable as a reference method. The samples were diluted 40 times prior to analysis so that measurements fell in the lineal range of the method.

RESULTS AND DISCUSSION

Wearable Device Part 1: Lactate Biosensor. The lactate biosensor features a unique design based on the flow of enzymes to a paper zone modified with a chromogen (Figure 1C). This was necessary because mixing enzymes and chromogens in the same reservoir spontaneously generated colorimetric signals in the absence of the analyte (Figure S5). While other designs rely on anchoring enzymes onto a transducer, in our prototype, the sample carries the enzyme to the detection zone, causing the enzyme concentration to change over time. Thus, the colorimetric signal varies as a function of the concentration of analyte, enzymatic activity, and sample volume. To better understand this signal generation mechanism, we first applied a fixed sample volume and measured changes in the signal originating from variations in the concentration of lactate. Figure 2A shows a photograph of the biosensors, which generate a blue hue caused by the oxidation of TMB. The colorimetric signal is linear in the concentration range between 0 and 1 mM. The limit of detection (LOD), expressed as the sample that yields a signal higher than 3 times the standard deviation of the blank, is 0.06 mM. To the best of our knowledge, this is the lowest LOD achieved with a colorimetric biosensor for sweat lactate detection and is comparable to electrochemical biosensors reported in the literature (Table S1).

While the design shown in Figure 2A has a low LOD, its dynamic range is not suitable for measuring variations of lactate in sweat.[33] In a healthy person, the sweat lactate concentration varies between 10 and 25 mM.[34] These values are much higher than the K_m value of LOX (0.15−1 mM), which means that the enzyme is saturated.[35] Therefore, it is not possible to obtain a dose-dependent response under these conditions (Figure S1A). Since reducing the concentration of analyte by diluting the sample was not an option, we devised a method for altering the K_m value of the enzyme and integrated it into the paper device. It consisted of storing a soluble competitive inhibitor, D-lactate, in several reservoirs of the paper biosensor.[35] The first reservoir (R1) was placed in a circular area close to the inlet mark. The second reservoir (R2) was the area containing the enzymes, as shown in Figure 1C. The configuration that yielded the best results in terms of linearity and sensitivity was adding two 1 μL drops of 1 M D-lactate in R1 and one 0.5 μL drop in R2 (Figures S6 and S7). Using these conditions, the biosensor yielded a concentration-dependent response in the range between 10 and 30 mM (Figure 2B). The limit of detection was 3.5 mM. Although this LOD is higher than in the previous configuration without an inhibitor, the redesigned biosensor is capable of measuring concentrations of lactate in the physiological range without the need for sample dilution. A full comparison with other reported methods is provided in Figure S8. While the biosensors can only yield semiquantitative measurements compared to the laboratory-based method in Figure S4, they are advantageous in that they allow one to estimate the levels of sweat lactate with minimal infrastructure on the spot. It has been shown that high increments in the concentration of sweat lactate (Δ5− 10 mM) may indicate risk to muscular tissues, hypoxia, or other conditions. Our prototypes are suitable for detecting such increments, and therefore they could be used to monitor these conditions at the point of need.[36] Primary sources of error are the instrumental error (smartphone camera) and differences in the paper fluidic devices related to the handmade manufacturing process. Using an automated paper cutting method and a piezoelectric dispenser for spotting reagents could reduce the fabrication error of future designs, thus improving the accuracy of the measurements.

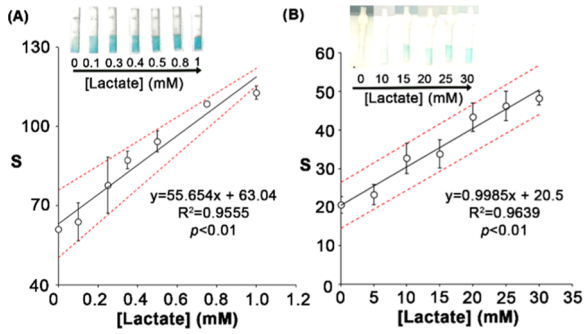

Figure 2. Calibration of lactate biosensor with a fixed sample volume (7 μL). (A) First-generation biosensors designed to obtain the lowest limit of detection (without inhibitor). (B) Second-generation biosensors tailored for quantifying lactate within the physiologically relevant concentration range. The error bars represent the standard deviation (SD, n = 3). S: colorimetric signal. The dotted red lines represent the 95% confidence interval of the calibration curves.

Wearable Device Part 2: Sweat Volume Sensor. The results shown in the previous section were obtained with a fixed sample volume. However, in real applications, the sweat volume entering the biosensor will change over time. Since the amount of enzyme arriving at the detection area depends on this parameter, the signal may change even when the concentration of lactate is the same. To correct this, the analytical platform shown in Figure 1A incorporates a sweat volume sensor based on the migration of gold nanoparticles. Figure 3A shows the images of the sensors after the addition of

https://dx.doi.org/10.1021/acssensors.0c01980
ACS Sens. 2021, 6, 130−136

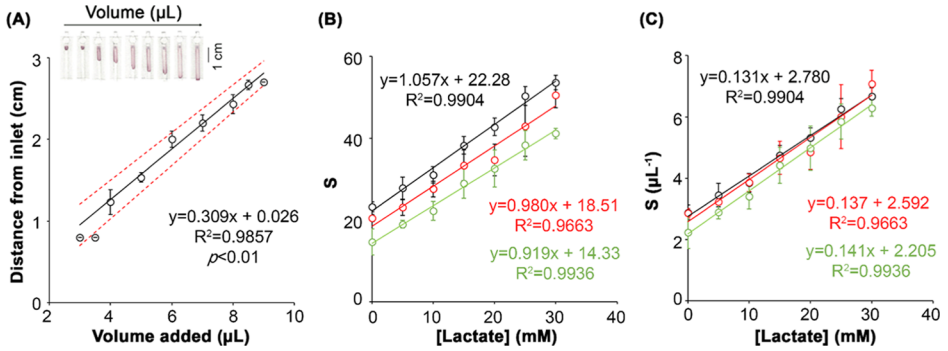

Figure 3. Sweat volume sensors. (A) Calibration as a function of different added volumes of PBS (3−9 μL). (B) Detection of L-lactate with different sample volumes: 6.5 μL (green), 7 μL (red), and 8 μL (black). (C) Detection of L-lactate after dividing the colorimetric lactate signal S by the sample volume measured with the sweat volume sensor (μL). The error bars represent the standard deviation (SD, n = 3). In (C), the error bars represent the propagated error of the lactate and volume measures. The red lines in (A) represent the 95% confidence interval.

controlled volumes of PBS to the inlet. The distance that the gold nanoparticles travel through the reservoir increases as the volume of added sample increases. The plot in Figure 3A shows that there is a linear relationship between these two parameters in the volume range between 4 and 8.5 μL. Lower volumes did not move the nanoparticles, while higher volumes surpassed the maximum length of the strip. However, it is important to note that the sensor design can be easily adapted to measure different volume ranges by adjusting the dimensions of the sensor (Figure S9). Below we explore how measuring the sample volume can be used to compensate for changes in the colorimetric signal originated by this parameter and improve the estimation of the lactate concentration.

Estimation of Lactate Levels with Varying Sample Volumes. Calibration curves for lactate using 6.5, 7, or 8 μL of sample were plotted to show the impact of varying sample volumes in the colorimetric signal generated by the lactate biosensor. In Figure 3B, the signal increases when more sample volume is added to the biosensor. The three calibration curves have similar slopes but different Y-intercepts, which indicates that the lactate signal is directly proportional to the added volume. Therefore, if the lactate signal was divided by the added volume, all calibration plots should yield the same result independently of this parameter. To demonstrate this hypothesis, the colorimetric signals of the lactate biosensor were divided by the sample volume calculated with the adjacent sensor depicted in Figure 1D and characterized in Figure 3A. Figure 3C shows the rectified calibration curves built with the normalized signal. To compare the calibration curves, the relative standard deviation (RSD, %) was calculated for each calibration point combining the three curves (n = 9 for each lactate concentration). For an individual concentration, a high RSD would mean that the three calibrations are different, while a low RSD would indicate that they are similar. Table 1 shows that the RSD values obtained with the corrected signals (S/V) are indeed low. This indicates that correcting the colorimetric signal S by the sample volume can reduce the effect of varying sample volumes in our lactate measures with an acceptable precision (RSD < 15%).[37] All in all, these experiments verify our initial hypothesis that the proposed analytical platform can quantify changes in the concentration of lactate even at different sample volumes thanks to combining lactate and volume measures.

Table 1. Relative Standard Deviation (RSD, %) of Each Calibration Point from Lactate Calibration Curve, Calculated Using All of the Replicates of Each Volume (6.5, 7, and 8 μL; n = 9)[a,b]

[lactate] (mM)	0	5	10	15	20	25	30
S/V	15	11	9.2	9.3	9.7	10	6.4

[a]S/V: volume-corrected colorimetric signal. [b]Volume-corrected detection of sweat lactate with the wearable analytical platform.

Finally, we tested our analytical platform when worn during physical exercise, as shown in Figure 4A. Five healthy volunteers were asked to perform a static cycling routine consisting of four different steps aimed at inducing changes in the concentration of sweat lactate. It should be noted that variations in these parameters may be different among the participants due to differences in fitness levels and age, among others.[33,38−40] Figure 4B−F shows the quantification of lactate levels during the exercise routine using the wearable analytical platform (red) or a reference method (black). Since skin temperature is higher than room temperature (controlled at 21 ± 2 °C), a calibration curve of sweat lactate was made at 37 °C to prevent a bias due to increased enzymatic activity in the wearable biosensors (Figure S10).

Volume-corrected measurements yield the same trend as the laboratory-based method for serial lactate measurements. The Bland−Altman plot in Figure 4G shows that, except for one outlier, all measures are inside the area representing a 95% agreement between the two methods (average difference, ± 1.96 SD). This demonstrates that our wearable device provides lactate measurements comparable to the reference method. It also shows a small bias (represented as a green line) since the values measured with our device were slightly higher than the measures with the reference method. Selectivity experiments indicate that glucose in the sample could be the origin of this small bias (Figure S11). Nevertheless, this bias was not statistically significant, indicating that the two methods yield equivalent measures (t test, p > 0.1). Lactate signals that were not corrected with the volume sensor yielded disparate values with a higher bias (Figure S16). Therefore, even though the volume entering adjacent sensors may be slightly different, combining the two sensors substantially improves the estimation of lactate levels. An anomalous performance of the device due to bending was discarded as well, since measures did not change significantly when the biosensors were bent up to 40° (Figure S13). Variations of sweat pH can affect the enzyme activity, and therefore could also increase the variability among experiments. In Figure S14, the devices

https://dx.doi.org/10.1021/acssensors.0c01980
ACS Sens. 2021, 6, 130−136

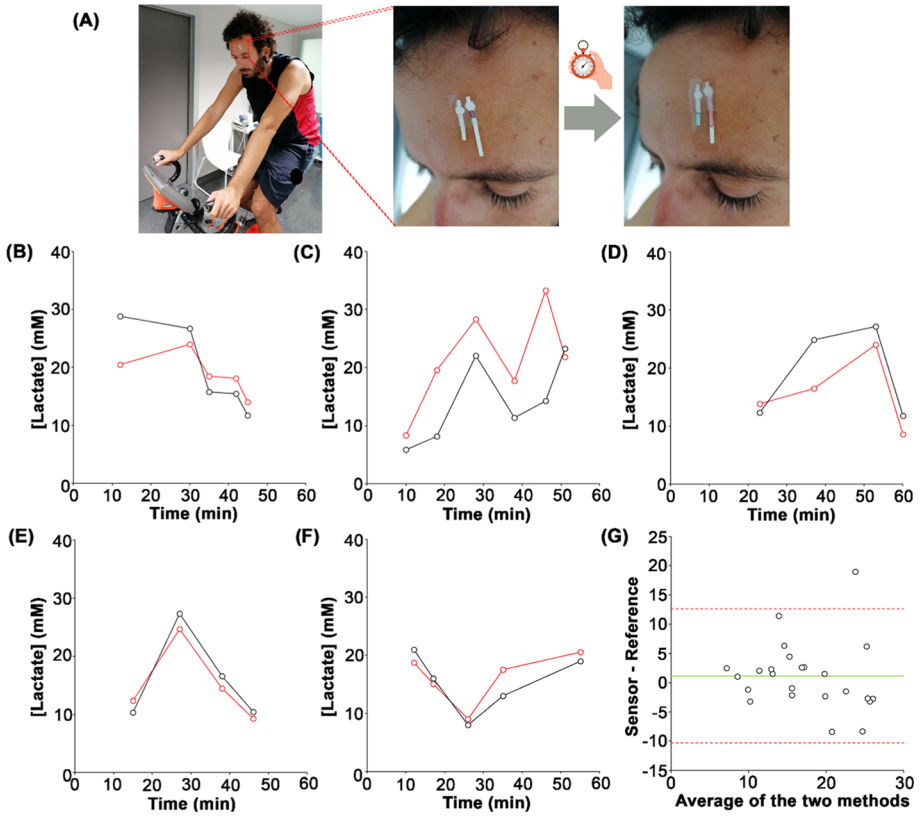

Figure 4. Volume-corrected sweat lactate measurements using the proposed wearable analytical platform. (A) Photographs showing the devices worn by a volunteer. (B–F) Lactate measures from five healthy volunteers at different time points. Sweat lactate concentrations were measured using either the wearable analytical platform, including volume corrections (red), or a laboratory-based method (black). (G) Bland–Altman plot representing all of the measures.

performed well when tested with artificial sweat samples at different pH values (5–7). Signals decreased slightly at pH 7 probably because the pH was not completely buffered by the supporting electrolyte (Figure S14). This could explain the different trend observed in the last point of Figure 4C. Future improvements of the device could feature a pH correction or a sensor array with multiple simultaneous lactate and volume measures to average errors and improve the precision and accuracy. In addition, an automatized fabrication procedure could reduce the manufacturing error. All things considered, our wearable prototypes are well suited to detect variations in lactate concentrations during exercise semiquantitatively.

CONCLUSIONS

In conclusion, a wearable analytical platform integrating a lactate biosensor and a sweat volume sensor for the semiquantitative measurement of sweat biomarkers is presented. The platform is made of small strips of filter paper, making it lightweight, easy to manufacture at any scale, and easy to dispose of, making it suitable as single-use wearable device. The sweat volume measure improves the quantification of lactate levels associated with different sweat rates. Furthermore, all of the components of the analytical platform are highly adaptable to fit different clinical and consumer preferences. For example, the dynamic range of the lactate biosensor can be tailored by adding an enzyme inhibitor. The sweat volume sensor can also be customized to measure changes in different volume ranges by adjusting the length and shape of the microfluidic design. The detection platform can be adapted to measure other biomarkers in sweat using different oxidoreductases as biorecognition elements, for example, uric acid using uricase. This, along with the highly customizable design, makes our approach a highly versatile platform for developing a wide array of wearable biosensors.

ASSOCIATED CONTENT

Supporting Information

The Supporting Information is available free of charge at https://pubs.acs.org/doi/10.1021/acssensors.0c01980.

AuNPs fabrication protocol; optimization of the LOX and TMB concentrations (Figure S1); effect of PSS concentration in nanoparticle flow (Figure S2); comparison between colorimetric signals obtained by photographing the biosensors with a scanner or a smartphone camera (Figure S3); spectrophotometric detection of L-lactate (Figure S4); spontaneous signal generation when storing enzymes and chromogens in the same reservoir (Figure S5); calibration plots obtained by adding different amounts of D-lactate in reservoirs 1 and/or 2 (Figure S6); D-lactate inhibition test (Figure S7); comparison of the dynamic ranges of the most relevant lactate wearable biosensors (Figure S8); fine-tuning the lineal range of the sweat volume sensor (Figure S9); lactate biosensor calibration at 37 °C (Figure S10); selectivity study (Figure S11); TMB mobilization test (Figure S12); bending (Figure S13); effect of pH (Figure S14); pore size (Figure S15); lactate measures without volume correction (Figure S16); and reported LODs for different sweat lactate

https://dx.doi.org/10.1021/acssensors.0c01980
ACS Sens. 2021, 6, 130–136

biosensors, calculated using the 3σ criterium (Table S1) (PDF)

AUTHOR INFORMATION

Corresponding Authors

Enrique Barón − *Multidisciplinary Sepsis Group, Health Research Institute of the Balearic Islands (IdISBa), Son Espases University Hospital, 07120 Palma de Mallorca, Spain;* orcid.org/0000-0001-7461-4599; Email: enrique.baron@ssib.es

Roberto de la Rica − *Multidisciplinary Sepsis Group, Health Research Institute of the Balearic Islands (IdISBa), Son Espases University Hospital, 07120 Palma de Mallorca, Spain;* orcid.org/0000-0002-5750-1469; Email: roberto.delarica@ssib.es

Author

Andreu Vaquer − *Multidisciplinary Sepsis Group, Health Research Institute of the Balearic Islands (IdISBa), Son Espases University Hospital, 07120 Palma de Mallorca, Spain*

Complete contact information is available at: https://pubs.acs.org/10.1021/acssensors.0c01980

Author Contributions

The manuscript was written through contributions of all authors. All authors have given approval to the final version of the manuscript.

Notes

The authors declare the following competing financial interest(s): R. R discloses that a patent application describing the method for storing nanoparticles in paper reservoirs has been filed (PCT/EP2020/075013).

ACKNOWLEDGMENTS

R.d.l.R. and E.B. acknowledge funding from IdISBa/Impost Turisme Sostenible/Agència d'Estratègia Turística de les Illes Balears-Govern de les Illes Balears through Radix and Folium fellowships, respectively. E.B. acknowledges funding from the Instituto de Salud Carlos III (Sara Borrell contract). A.V. acknowledges funding from European Social Fund (ESF) through JoTReSdOS program.

REFERENCES

(1) Koh, A.; Kang, D.; Xue, Y.; Lee, S.; Pielak, R. M.; Kim, J.; Hwang, T.; Min, S.; Banks, A.; Bastien, P.; Manco, M. C.; Wang, L.; Ammann, K. R.; Jang, K. I.; Won, P.; Han, S.; Ghaffari, R.; Paik, U.; Slepian, M. J.; Balooch, G.; Huang, Y.; Rogers, J. A. A Soft, Wearable Microfluidic Device for the Capture, Storage, and Colorimetric Sensing of Sweat. *Sci. Transl. Med.* **2016**, *8*, No. 366ra165.

(2) Choi, J.; Bandodkar, A. J.; Reeder, J. T.; Ray, T. R.; Turnquist, A.; Kim, S. B.; Nyberg, N.; Hourlier-Fargette, A.; Model, J. B.; Aranyosi, A. J.; Xu, S.; Ghaffari, R.; Rogers, J. A. Soft, Skin-Integrated Multifunctional Microfluidic Systems for Accurate Colorimetric Analysis of Sweat Biomarkers and Temperature. *ACS Sens.* **2019**, *4*, 379−388.

(3) He, X.; Xu, T.; Gao, W.; Xu, L. P.; Pan, T.; Zhang, X. Flexible Superwettable Tapes for On-Site Detection of Heavy Metals. *Anal. Chem.* **2018**, *90*, 14105−14110.

(4) Kim, J.; Campbell, A. S.; de Ávila, B. E. F.; Wang, J. Wearable Biosensors for Healthcare Monitoring. *Nat. Biotechnol.* **2019**, *37*, 389−406.

(5) Guk, K.; Han, G.; Lim, J.; Jeong, K.; Kang, T.; Lim, E. K.; Jung, J. Evolution of Wearable Devices with Real-Time Disease Monitoring for Personalized Healthcare. *Nanomaterials* **2019**, *9*, No. 813.

(6) Tricoli, A.; Nasiri, N.; De, S. Wearable and Miniaturized Sensor Technologies for Personalized and Preventive Medicine. *Adv. Funct. Mater.* **2017**, *27*, No. 1605271.

(7) Oncescu, V.; O'Dell, D.; Erickson, D. Smartphone Based Health Accessory for Colorimetric Detection of Biomarkers in Sweat and Saliva. *Lab Chip* **2013**, *13*, 3232−3238.

(8) Gualandi, I.; Tessarolo, M.; Mariani, F.; Cramer, T.; Tonelli, D.; Scavetta, E.; Fraboni, B. Nanoparticle Gated Semiconducting Polymer for a New Generation of Electrochemical Sensors. *Sens. Actuators, B* **2018**, *273*, 834−841.

(9) He, X.; Yang, S.; Pei, Q.; Song, Y.; Liu, C.; Xu, T.; Zhang, X. Integrated Smart Janus Textile Bands for Self-Pumping Sweat Sampling and Analysis. *ACS Sens.* **2020**, *5*, 1548−1554.

(10) Sekine, Y.; Kim, S. B.; Zhang, Y.; Bandodkar, A. J.; Xu, S.; Choi, J.; Irie, M.; Ray, T. R.; Kohli, P.; Kozai, N.; Sugita, T.; Wu, Y.; Lee, K.; Lee, K. T.; Ghaffari, R.; Rogers, J. A. A Fluorometric Skin-Interfaced Microfluidic Device and Smartphone Imaging Module for: In Situ Quantitative Analysis of Sweat Chemistry. *Lab Chip* **2018**, *18*, 2178−2186.

(11) Choi, J.; Ghaffari, R.; Baker, L. B.; Rogers, J. A. Skin-Interfaced Systems for Sweat Collection and Analytics. *Sci. Adv.* **2018**, *4*, No. eaar3921.

(12) Rachim, V. P.; Chung, W. Y. Wearable-Band Type Visible-near Infrared Optical Biosensor for Non-Invasive Blood Glucose Monitoring. *Sens. Actuators, B* **2019**, *286*, 173−180.

(13) Bae, S. H.; Kim, D.; Chang, S. Y.; Hur, J.; Kim, H.; Lee, J. W.; Zhu, B.; Han, T. H.; Choi, C.; Huffaker, D. L.; Di Carlo, D.; Yang, Y.; Rim, Y. S. Hybrid Integrated Photomedical Devices for Wearable Vital Sign Tracking. *ACS Sens.* **2020**, *5*, 1582−1588.

(14) Sempionatto, J. R.; Khorshed, A. A.; Ahmed, A.; De Loyola e Silva, A. N.; Barfidokht, A.; Yin, L.; Goud, K. Y.; Mohamed, M. A.; Bailey, E.; May, J.; Aebischer, C.; Chatelle, C.; Wang, J. Epidermal Enzymatic Biosensors for Sweat Vitamin C: Toward Personalized Nutrition. *ACS Sens.* **2020**, *5*, 1804−1813.

(15) Cao, Q.; Liang, B.; Tu, T.; Wei, J.; Fang, L.; Ye, X. Three-Dimensional Paper-Based Microfluidic Electrochemical Integrated Devices (3D-PMED) for Wearable Electrochemical Glucose Detection. *RSC Adv.* **2019**, *9*, 5674−5681.

(16) He, X.; Pei, Q.; Xu, T.; Zhang, X. Smartphone-Based Tape Sensors for Multiplexed Rapid Urinalysis. *Sens. Actuators, B* **2020**, *304*, No. 127415.

(17) Liu, C.; Xu, T.; Wang, D.; Zhang, X. The Role of Sampling in Wearable Sweat Sensors. *Talanta* **2020**, *212*, No. 120801.

(18) He, X.; Xu, T.; Gu, Z.; Gao, W.; Xu, L. P.; Pan, T.; Zhang, X. Flexible and Superwettable Bands as a Platform toward Sweat Sampling and Sensing. *Anal. Chem.* **2019**, *91*, 4296−4300.

(19) Morbioli, G. G.; Mazzu-Nascimento, T.; Stockton, A. M.; Carrilho, E. Technical Aspects and Challenges of Colorimetric Detection with Microfluidic Paper-Based Analytical Devices (MPADs) - A Review. *Anal. Chim. Acta* **2017**, *970*, 1−22.

(20) Gong, M. M.; Sinton, D. Turning the Page: Advancing Paper-Based Microfluidics for Broad Diagnostic Application. *Chem. Rev.* **2017**, *117*, 8447−8480.

(21) Akyazi, T.; Basabe-Desmonts, L.; Benito-Lopez, F. Review on Microfluidic Paper-Based Analytical Devices towards Commercialisation. *Anal. Chim. Acta* **2018**, *1001*, 1−17.

(22) Ray, T. R.; Choi, J.; Bandodkar, A. J.; Krishnan, S.; Gutruf, P.; Tian, L.; Ghaffari, R.; Rogers, J. A. Bio-Integrated Wearable Systems: A Comprehensive Review. *Chem. Rev.* **2019**, *119*, 5461−5533.

(23) López-Marzo, A. M.; Merkoçi, A. Paper-Based Sensors and Assays: A Success of the Engineering Design and the Convergence of Knowledge Areas. *Lab Chip* **2016**, *16*, 3150−3176.

(24) Martinez, A. W.; Phillips, S. T.; Whitesides, G. M.; Carrilho, E. Diagnostics for the Developing World: Microfluidic Paper-Based Analytical Devices. *Anal. Chem.* **2010**, *82*, 3−10.

(25) Jang, H.; Park, J. H.; Oh, J.; Kim, K.; Kim, M. G. Advanced Colorimetric Paper Sensors Using Color Focusing Effect Based on Asymmetric Flow of Fluid. *ACS Sens.* **2019**, *4*, 1103−1108.
(26) Dam, V. A. T.; Zevenbergen, M. A. G.; van Schaijk, R. Toward Wearable Patch for Sweat Analysis. *Sens. Actuators, B* **2016**, *236*, 834−838.
(27) Lin, H.; Tan, J.; Zhu, J.; Lin, S.; Zhao, Y.; Yu, W.; Hojaiji, H.; Wang, B.; Yang, S.; Cheng, X.; Wang, Z.; Tang, E.; Yeung, C.; Emaminejad, S. A Programmable Epidermal Microfluidic Valving System for Wearable Biofluid Management and Contextual Biomarker Analysis. *Nat. Commun.* **2020**, *11*, No. 4405.
(28) Nyein, H. Y. Y.; Tai, L. C.; Ngo, Q. P.; Chao, M.; Zhang, G. B.; Gao, W.; Bariya, M.; Bullock, J.; Kim, H.; Fahad, H. M.; Javey, A. A Wearable Microfluidic Sensing Patch for Dynamic Sweat Secretion Analysis. *ACS Sens.* **2018**, *3*, 944−952.
(29) Martín, A.; Kim, J.; Kurniawan, J. F.; Sempionatto, J. R.; Moreto, J. R.; Tang, G.; Campbell, A. S.; Shin, A.; Lee, M. Y.; Liu, X.; Wang, J. Epidermal Microfluidic Electrochemical Detection System: Enhanced Sweat Sampling and Metabolite Detection. *ACS Sens.* **2017**, *2*, 1860−1868.
(30) Parrilla, M.; Guinovart, T.; Ferré, J.; Blondeau, P.; Andrade, F. J. A Wearable Paper-Based Sweat Sensor for Human Perspiration Monitoring. *Adv. Healthcare Mater.* **2019**, *8*, No. 1900342.
(31) Alba-Patiño, A.; Adrover-Jaume, C.; La Rica, R. D. Nanoparticle Reservoirs for Paper-Only Immunosensors. *ACS Sens.* **2020**, *5*, 147−153.
(32) Derbyshire, P. J.; Barr, H.; Davis, F.; Higson, S. P. J. Lactate in Human Sweat: A Critical Review of Research to the Present Day. *J. Physiol. Sci.* **2012**, *62*, 429−440.
(33) Seshadri, D. R.; Li, R. T.; Voos, J. E.; Rowbottom, J. R.; Alfes, C. M.; Zorman, C. A.; Drummond, C. K. Wearable Sensors for Monitoring the Physiological and Biochemical Profile of the Athlete. *npj Digit. Med.* **2019**, *2*, No. 72.
(34) Alam, F.; RoyChoudhury, S.; Jalal, A. H.; Umasankar, Y.; Forouzanfar, S.; Akter, N.; Bhansali, S.; Pala, N. Lactate Biosensing: The Emerging Point-of-Care and Personal Health Monitoring. *Biosens. Bioelectron.* **2018**, *117*, 818−829.
(35) Streitenberger, S. A.; López-Mas, J. A.; Sánchez-Ferrer, Á.; García-Carmona, F. Non-Linear Slow-Binding Inhibition of *Aerococcus viridans* Lactate Oxidase by Cibacron Blue 3GA. *J. Enzyme Inhib.* **2001**, *16*, 301−312.
(36) Karpova, E. V.; Laptev, A. I.; Andreev, E. A.; Karyakina, E. E.; Karyakin, A. A. Relationship Between Sweat and Blood Lactate Levels During Exhaustive Physical Exercise. *ChemElectroChem* **2020**, *7*, 191−194.
(37) Mendes, N. S.; Pereira, S. M. F.; Arantes, M. B. S.; Glória, L. L.; Nunes, C. R.; de Passos, M. S.; Vieira, I. J. C.; de Moraes, L. P.; Rodrigues, R.; Oliveira, D. B. Bioanalytical Method Validation for the Quantification of the Chlorogenic Acid in Capsicum Baccatum through High Performance Liquid Chromatography (HPLC-DAD). *Food Chem.* **2020**, *325*, No. 126929.
(38) Sakharov, D. A.; Shkurnikov, M. U.; Vagin, M. Y.; Yashina, E. I.; Karyakin, A. A.; Tonevitsky, A. G. Relationship between Lactate Concentrations in Active Muscle Sweat and Whole Blood. *Bull. Exp. Biol. Med.* **2010**, *150*, 83−85.
(39) Buono, M. J.; Lee, N. V. L.; Miller, P. W. The Relationship between Exercise Intensity and the Sweat Lactate Excretion Rate. *J. Physiol. Sci.* **2010**, *60*, 103−107.
(40) Zhang, Q.; Jiang, D.; Xu, C.; Ge, Y.; Liu, X.; Wei, Q.; Huang, L.; Ren, X.; Wang, C.; Wang, Y. Wearable Electrochemical Biosensor Based on Molecularly Imprinted Ag Nanowires for Noninvasive Monitoring Lactate in Human Sweat. *Sens. Actuators, B* **2020**, *320*, No. 128325.

https://dx.doi.org/10.1021/acssensors.0c01980
ACS Sens. 2021, 6, 130−136